

# Development of a Fluidized Bed Thermogravimetric Analyzer

Said Samih and Jamal Chaouki

Dept. of Chemical Engineering, École Polytechnique de Montreal, PO Box 6079, Succ. Centre-ville, Montréal, QC H3C 3A7, Canada

DOI 10.1002/aic.14637

Published online October 12, 2014 in Wiley Online Library (wileyonlinelibrary.com)

A new fluidized bed thermogravimetric analyzer (FB-TGA) was developed that introduces two major particularities: the pseudo variation of the weight of the reactor and the special strategy for gas flow rate adjustment according to temperature. A momentum balance was performed on the reactor and the pseudo variation of the reactor weight was evaluated by measuring the pressure drop through the gas distributor and filter. The real weight loss of the reactor was obtained by subtracting the pseudo variation of the weight from the total weight loss measured by the load cell. In addition, a special program for the gas flow rate as a function of temperature was developed and used; so the minimum fluidization regime is maintained throughout all of the experiments. The validation test of the FB-TGA was carried out on calcium hydroxide decomposition, and the results were compared with those obtained from the conventional TGA. Diffusion control was suppressed by the application of the FB-TGA, which was confirmed by the x-ray diffraction analysis on the treated samples. © 2014 American Institute of Chemical Engineers *AIChE J.* 61: 84–89, 2015

**Keywords:** fluidized bed thermogravimetric analyzer, fluidized bed TGA, kinetics, gas-solid reactions, fluidization

## Introduction

The kinetics and mechanism of thermally activated catalytic gas-solid reactions are usually obtained from thermal gravimetry analysis (TGA), differential thermal analysis, and differential scanning calorimetry.<sup>1–6</sup> These experimental techniques have been commonly applied to characterize a wide range of reactions, such as solid fuels pyrolysis, gasification and combustion,<sup>7–11</sup> thermal decomposition of different materials,<sup>3,4,7</sup> crystallization of polymers, regeneration of deactivated catalysts, and oxidation-reduction of metal oxides.<sup>11,12</sup>

In spite of a wide range of applications in academia and the industry, the thermogravimetric (TG) technique shows some limitations, which may reduce the reliability of kinetic models. In more concrete terms, studying kinetics in the conventional TGA suffers seriously from (1) the nonuniformity of the temperature throughout the sample, (2) poor mixing and distribution of gas-solid and solid-solid throughout the sample, (3) the low heating rate, (4) the small amount of solid sample, which is not enough to represent its homogeneity, (5) and the bulk, interparticle, and intraparticle diffusion control.<sup>1,13</sup>

Recently, our research group investigated the diffusional effects in TGA during the oxidation of SiC powders under air (gas reactant) in a cylindrical crucible.<sup>13</sup> In general, in

the gas-solid reaction, four types of regimes can control the reaction rate (Figure 1) according to the experimental configuration: (1) intradiffusion (diffusion of the gaseous reactant through the product layer) and surface reaction, (2) bulk diffusion (diffusion of the gaseous reactant from the bulk to the surface of the bed), intradiffusion, and surface reaction, (3) interparticle diffusion (diffusion through the pore space between particles), intradiffusion, and surface reaction, and finally, (4) bulk, interdiffusion, and intradiffusion, and surface reaction. Depending on the mechanism of the reaction and physical properties of the system, such as porosity and height of the system (crucible), these diffusional steps may limit separately or simultaneously the overall reaction.

To overcome these issues and offer accurate and more comprehensive kinetic models, a new fluidized bed thermogravimetric analyzer (FB-TGA) was developed. Consequently, due to the proper mixing and the uniform distribution of gas-solid and solid-solid that fluidization provides, the fluidized bed reaction chamber can easily ensure (1) the uniformity of the temperature throughout the sample, (2) the use of a sufficient amount of the solid sample, (3) the real elimination of the bulk and interparticle diffusion controls, and (4) the use of a higher heating rate, which can represent the reality of what is happening in catalytic gas-solid reactions on an industrial scale. Moreover, by playing with the solid inerts and reactant particle size, the intraparticle diffusion control could be partially suppressed.

The primary application of the newly developed equipment was carried out on calcium hydroxide decomposition. The results obtained were compared with those obtained from the conventional TGA.

Additional Supporting Information may be found in the online version of this article.

Correspondence concerning this article should be addressed to J. Chaouki at jamal.chaouki@polymtl.ca.

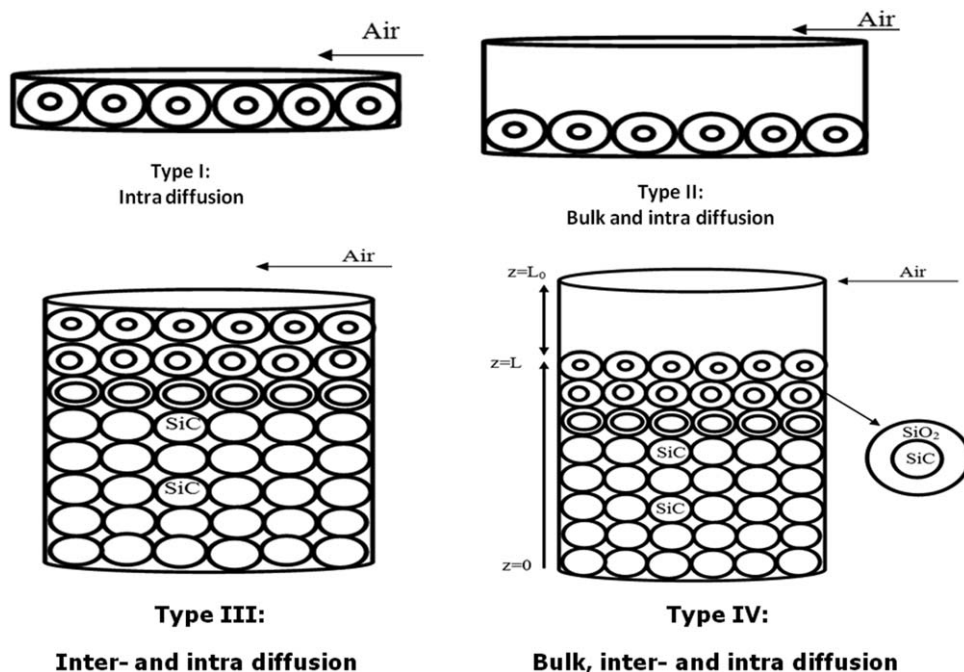


Figure 1. Different types of diffusion. Reproduced with permission from Ebrahimpour et al., J Mater Sci, 2013, 48, 4396–4407.

## Apparatus Description

As shown in Figure 2, the fluidized bed reactor (FB-TGA) includes three main parts: the microreactor, the furnace, and the various measuring instruments. The quartz fluidized bed reactor measures 1 in. in diameter and 6 in. in length (or height). The measuring instruments consist of (1) a load cell for weight measurement, (2) a thermocouple for temperature measurement of the bed, (3) pressure transducers for pressure drop measurement, and (4) two mass flow controllers (MFCs) for gas flow rate adjustment depending on the temperature. The equipment is linked to a data acquisition system and the gas outlet is connected to a GC/FT-IR system.

Furthermore, software was developed for the FB-TGA to keep the system at approximately minimum fluidization at

any temperature. The software includes a program for gas flow rates as a function of temperature. Also, the two MFCs are linked to the thermocouple, which permits decreasing the gas flow rates when the temperature is increasing.

## Concept of the “pseudo variation” of the weight of the fluidized bed TGA

Figure 3 illustrates the concept of the pseudo variation of the weight of the reactor. As shown in this curve, two zones can be identified as follows: (1) the first one where the reactor was empty, so the mass of sand was 0 g, and (2) the second zone where 25 g of sand was used in the bed. For the two experiments, three different gas velocities were tested:  $U_g = 0 U_{mf}$ ,  $U_g = U_{mf}$ , and  $U_g = 1.25 U_{mf}$ . The results suggest that the whole weight of the reactor decreases when the gas velocity increases. Thus, when the gas velocity changes from  $0 U_{mf}$  to  $U_{mf}$ , the variation of the weight of the reactor

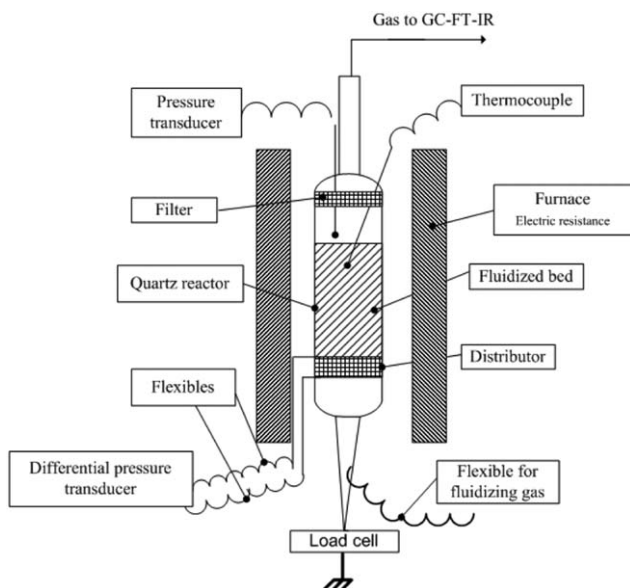


Figure 2. Schematic of the Fluidized Bed TGA.

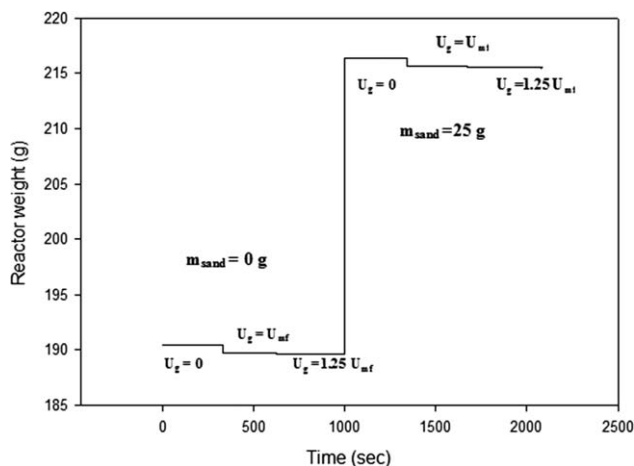


Figure 3. Pseudo variation of the reactor weight: Mass of sand = 0; 25 g.

remains the same for the two different masses of sand; 0 g and 25 g. The same conclusion was observed by changing the gas velocity from  $U_{mf}$  to  $1.25 U_{mf}$ .

Regarding this experimental conclusion, the measured weight of the reactor or apparent weight could be described by Eq. 1

$$m_{app} = m_{real} - \Delta m_p \quad (1)$$

where  $m_{app}$  and  $m_{real}$  represent the apparent and real weight of the reactor and  $\Delta m_p$  denotes the variation of the weight of the reactor.

This “pseudo variation” of the weight of the reactor, shown in Figure 2, is due to the pressure drop through the distributor and filter. Modeling the pseudo variation of the weight of the fluidized bed reactor will be developed in the next section.

### Modeling the pseudo variation of the weight of the reactor

**Momentum Balance on the Reactor.** It is important to keep the fluidization regime at “around” minimum to (1) profit from the fluidization advantages and to avoid (2) the vibration effect of fluidization on weight measurement, and (3) the hydrodynamics effect on the study of kinetics.

Nevertheless, the gas and the minimum fluidization velocities change with the temperature. Hence, the control and regulation of the gas flow rate with the temperature is necessary to keep the system near the minimum fluidization regime. For this reason, the FB-TGA is equipped with two (2) MFC. Using a special program, the MFCs adjust the gas flow rate instantaneously when the temperature increases.

Conversely, by changing the gas velocity, the pressure drop through the distributor and filter will be affected. Therefore, modeling the pseudo variation of the weight of the reactor is required.

By performing a momentum balance on the micro-fluidized bed reactor, and neglecting the convection term and the weight of the fluid inside the reactor, the force applied by the fluidizing gas on the reactor can be expressed as follows

$$F_{\text{fluid} \rightarrow \text{reactor}}|_z = (\Delta P_{\text{dist.}} + \Delta P_{\text{filter}}) \times S \quad (2)$$

Hence, the pseudo variation of the weight of the reactor is due to the force expressed by Eq. 2. Therefore, Eq. 3 gives the expression of the “pseudo variation of the weight of the reactor,” denoted  $\Delta m_p$ , as a function of the pressure drop across the distributor and filter of the reactor

$$\Delta m_p = \alpha_p \times (\Delta P_{\text{dist.}} + \Delta P_{\text{filter}}); \alpha_p = \frac{S}{g} \quad (3)$$

Furthermore, the apparent weight of the reactor, which is measured by the load cell, can be expressed by Eq. 4

$$m_{app.}(t, T, U_g) = m_{real}(t, T, U_g) - \Delta m_p(t, T, U_g) \quad (4)$$

where

$$m_{real}(t, T, U_g) = m_{\text{reactor}}(t, T, U_g) + m_{\text{bed}}(t, T) \quad (5)$$

and  $\Delta m_p$  denotes the pseudo variation of the reactor weight that is given by Eq. 3.

In more concrete terms, the model gives the real weight of the reactor in the fluidized bed TGA is expressed in Eq. 6

$$m_{real}(t, T, U_g) = m_{app.}(t, T, U_g) + \Delta m_p(t, T, U_g) \quad (6)$$

To include the effect of the pseudo variation of the reactor weight in the FB-TGA results, the pressure drop along dis-

tributer and filter should be measured, converted to weight, and subtracted from the total weight loss of the reactor.

### Experimental Procedures

For the experiments shown in Figure 3, which illustrates the concept of the pseudo variation of the reactor weight in the FB-TGA, the used fluidizing agent was air. The experiments were carried out at 25°C (room temperature), and 0 g and 25 g of sand were used. The minimum fluidization velocity was determined by measuring the pressure drop across the bed.

However, for the validation of the pseudo variation of the weight at ambient temperature, two different strategies were used. For the results represented in Figure 4, it was proposed to validate that the pseudo variation of the weight, explained above in the article, is only due to the pressure drop across the distributor. Therefore, according to the Ergun equation, which gives the pressure drop as a function of the square of the gas velocity ( $\Delta P \propto U_g^2$ ) for the turbulent regime, this experimental pseudo variation of the weight should follow the same law. Hence, by changing the fluidizing gas velocity and measuring the weight of the reactor by the load cell, the experimental resulting weight loss of the reactor should be proportional to the square of the gas velocity ( $\Delta m \propto U_g^2$ ). It should be indicated that, during the experiments presented in Figure 4, different masses of sand were tested (0 g, 10 g, 20 g, and 30 g) and there was no filter at the top of the reactor.

As indicated in Figure 4, the results were modeled and the model is:  $\Delta m = 0.0025 U_g^2$ . It should be remembered that the model shown in Figure 4 is completely different from the one mentioned in Figure 5.

Furthermore, Figure 5 (Measuring the weight of the bed: Model vs. Bed pressure drop) indicates the second strategy for confirmation and validation, at ambient temperature, that the pseudo variation of the reactor weight is due to the pressure drop along the distributor and filter of the reactor. For these experiments, the fluidizing agent used was air and 20 g of tested sand. The air velocity was changing and three parameters were measured: (1) the weight of the reactor that was measured by the load cell, (2) the pressure drop along the distributor, and (3) the pressure drop across the bed. The load cell indicates the apparent bed weight that is corrected by the model, which gives the pseudo variation of the reactor as a function of pressure drop along the distributor (Eqs. 3 and 6). The results are shown in Figure 5 (Real bed weight [model]). Moreover, the pressure drop across the bed was converted to weight that is illustrated by Figure 5 (Bed weight [bed pressure drop]). The initial weight of the bed (20 g) is shown in Figure 5 (Bed weight [sample]). Finally, it should be indicated that the FB-TGA operates at ambient pressure and the pressure drop across the filter is negligible.

For the section (pseudo variation of the weight: validation at high temperature), three different masses of sand were tested: 20, 25, and 30 g. For all experiments, the fluidizing agent used was air and the reactor heated up according to the following temperature profile: (1) isothermal for 10 min at 25°C (ambient temperature), (2) temperature ramp rate of 20°C/min up to 600°C, and (3) isothermal for 20 min at 600°C. The values of minimum fluidization velocities, at different temperatures, were determined by measuring the pressure drop of the bed at the corresponding temperatures. The corresponding gas flow rate for the minimum fluidization regime, at different temperatures, was used as shown in Figure 6 (Gas flow rate adjustment vs. temperature).

At any temperature, the load cell measures the apparent weight of the reactor and the pressure transducer gives the pressure drop across the distributor. The results are given in Figure 8. The apparent weight, which is obtained from the load cell, is corrected by the model giving the pseudo variation of the reactor weight as a function of the pressure drop along the distributor (Eqs. 3 and 6). For the different masses of sand used, the obtained results are shown in Figure 8 (corrected weight from the model (20–25–30 g). The bed weights obtained from the pressure drop across the bed are also represented in Figure 8 (bed weight from the bed pressure drop).

For the section (Experimental validation: calcium hydroxide decomposition), the experiments were carried out in argon (Ar) atmosphere and according to the following temperature profile: (1) isothermal for 10 min at 25°C (ambient temperature), (2) temperature ramp rate of 20°C/min up to 650°C, and (3) isothermal for 30 min at 650°C. The conventional TGA that was used for the experiments presented in Figure 9 was the TGA Q-50 instrument type. Three (03) different masses of calcium hydroxide were tested: 10, 25, and 140 mg. The mean particle size of  $\text{Ca}(\text{OH})_2$  was 45  $\mu\text{m}$  and the particle density was 2340  $\text{kg m}^{-3}$ . However, for the decomposition of calcium hydroxide in the fluidized bed TGA, 4 g of  $\text{Ca}(\text{OH})_2$  was mixed with 30 g of sand. The mean particle size was 45  $\mu\text{m}$  for  $\text{Ca}(\text{OH})_2$  and 75  $\mu\text{m}$  for sand. The particle density for the sand used was 2650  $\text{kg m}^{-3}$  while the one for  $\text{Ca}(\text{OH})_2$  was 2340  $\text{kg m}^{-3}$ .

The values of minimum fluidization velocities of the mixture were calculated by measuring the bed pressure drop at different temperatures. Also, two thermocouples were used, at different  $z$  and  $r$  positions in the fluidized bed, to confirm that the bed was well fluidized at all times during the experiments.

#### **Pseudo variation of the weight: Validation at ambient temperature**

It is well known that the pressure drop across the distributor is proportional to the square of the gas velocity ( $\Delta P_{\text{distr.}} \propto U_g^2$ ). For confirmation and validation of the model converting the pressure drop of the distributor into reactor weight loss, experiments were carried out at ambient temperature and the results are shown in Figures 4 and 5.

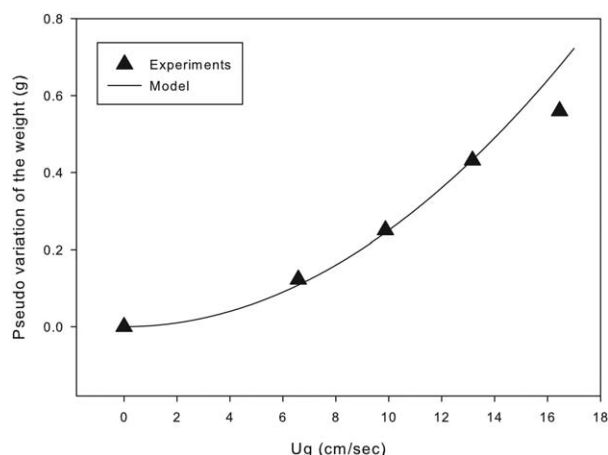


**Figure 4. Modeling the pseudo variation of the reaction weight: Validation ( $T = 25^\circ\text{C}$ ).**

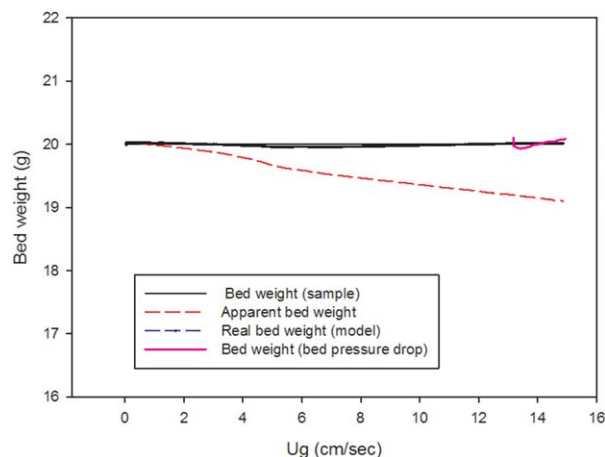


**Figure 5. Measuring the weight of the bed: Model vs. Bed pressure drop.**

[Color figure can be viewed in the online issue, which is available at [wileyonlinelibrary.com](http://wileyonlinelibrary.com).]

It should be indicated that, depending on the particle size of the fluidization material, the gas velocity for the experiments could range from 2 to 14 cm/s.

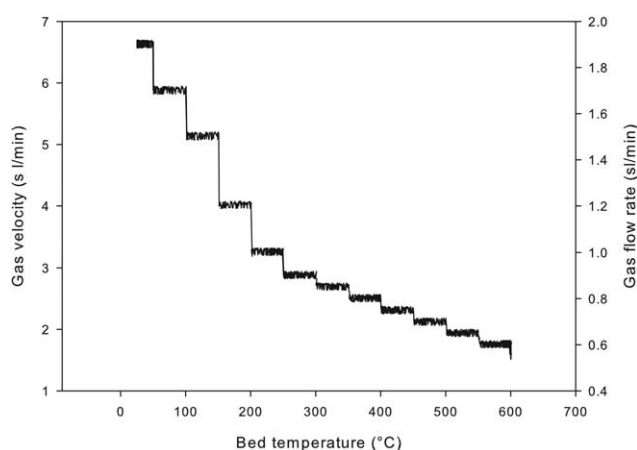
Moreover, the bed weight measured by the pressure drop of the bed shows some fluctuations, contrary to that obtained from the model. The validation of the model at high temperature is given in the next section.

#### **Pseudo variation of the weight: Validation at high temperature**

The objectives of this section focus on validating the modeling of the pseudo variation of the reactor weight at high temperature and the use and confirmation of the strategy for the gas flow rate adjustment vs. temperature.

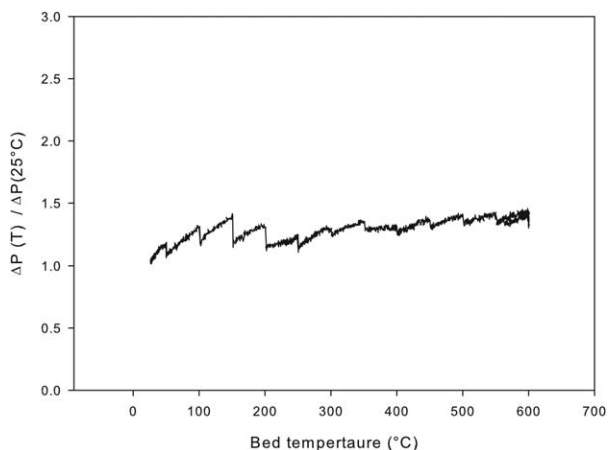
Figure 6 shows the flow rate adjustment vs. temperature. The gas flow rate decreases when the temperature is increasing and remains constant for each 50°C segment of temperature. This segment of temperature was chosen so that the fluidization regime remains steady at around minimum fluidization.

Figure 7 illustrates the variation in pressure drop throughout the distributor depending on the temperature. For each 50°C segment of temperature where the temperature remains



**Figure 6. Gas flow rate adjustment vs. temperature.**





**Figure 7. Pressure drop vs. temperature.**

constant, the pressure drop increases gradually. When the gas flow rate decreases, however, the pressure drop decreases instantaneously.

The validation, at high temperature, of the model developed for the pseudo variation of the reactor weight is demonstrated in Figure 8. The reactor for the FB-TGA was tested with three different masses of sand: 20, 25, and 30 g. The heating rate was 20°C/min and the reactor was heated up to 600°C.

The obtained results suggest that the weight of the reactor decreases roughly with the temperature. By converting the value of the pressure drop throughout the distributor, the corrected weight of the reactor (bed), according to the developed model, remained constant with the temperature.

Hence, using these strategies, the weight loss due to thermal transformation is measured precisely, which makes the developed FB-TGA an accurate standard piece of equipment for the kinetics study of catalytic gas-solid reactions.

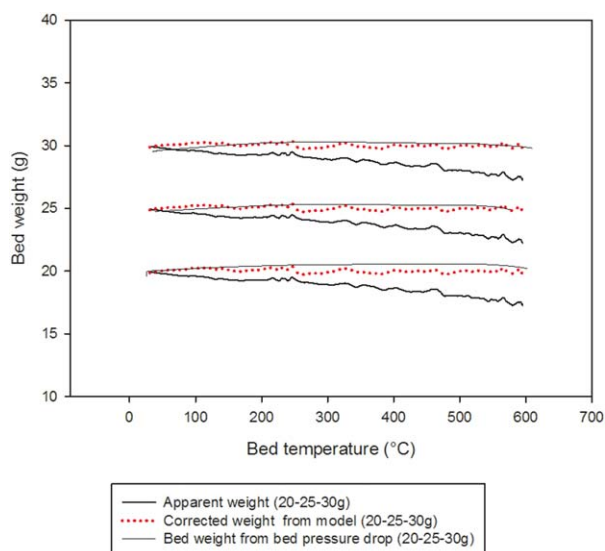


**Figure 8. Pseudo variation of weight vs. temperature.**

[Color figure can be viewed in the online issue, which is available at [wileyonlinelibrary.com](http://wileyonlinelibrary.com).]

### Experimental validation: Calcium hydroxide decomposition

Application and validation of the newly developed fluidized bed TGA were carried out on the calcium hydroxide ( $\text{Ca}(\text{OH})_2$ ) decomposition. The validation tests were done in an Argon (Ar) atmosphere with a heating rate of 20°C/min. The results obtained from the conventional TGA and the FB-TGA are shown in Figure 9.

Three (3) amounts of  $\text{Ca}(\text{OH})_2$  were tested on the conventional TGA: 10 and 25 mg to validate that there is no diffusion (bulk and interparticle) control and 140 mg to demonstrate the diffusion limitation on the conventional TGA. However, 4 g of  $\text{Ca}(\text{OH})_2$  were tested on the FB-TGA to confirm that there is no diffusion control limitation.

For the conventional TGA, the results obtained for 10 and 25 mg are similar but different from those obtained for 140 mg. The obtained curves can be divided into two major parts, denoting two different reaction stages. The first zone can be represented by 370–470°C for 10 and 25 mg and 395–565°C for 140 mg while the second zone can be delimited by 470–650°C for 10 and 25 mg and 565–650°C for 140 mg.

The overall process of conversion of solid  $\text{Ca}(\text{OH})_2$  into  $\text{CaO}$  and water vapor, involving the subprocesses of heat transfer, mass transfer, and thermal decomposition kinetics, is driven by the rate of thermal energy flux received by the inner core of  $\text{Ca}(\text{OH})_2$  surrounded by the shell of  $\text{CaO}(\text{s})$  in a solid (say) spherical particle. For a given particle, the product species, water vapor would issue out of the particle through pores in the core of  $\text{Ca}(\text{OH})_2$  and shell of  $\text{CaO}$  in the form of jets (involving convective flow due to the build-up of pressure gradient between the particle interior and its exterior surface) or via the Knudsen/bulk molecular diffusion depending on the rate of thermal energy flux and particle pore size.

Accordingly, during the first stage, the difference shown between the results obtained from 10–25 mg and 140 mg is due to the heat transfer limitation and/or the temperature gradient throughout the sample (140 mg). Nevertheless, the intraparticle diffusion of  $\text{H}_2\text{O}$  through a small layer of  $\text{CaO}$  that was formed around the  $\text{Ca}(\text{OH})_2$  particle and, its external diffusion through the gas film around the particle, gradually became the rate-controlling step of the thermal decomposition reaction during the second part.

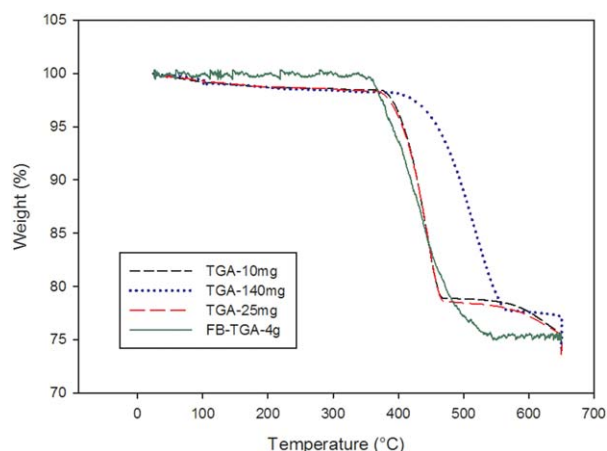


**Figure 9.  $\text{Ca}(\text{OH})_2$  decomposition: Comparison between Conventional and Fluidized Bed TGAs.**

[Color figure can be viewed in the online issue, which is available at [wileyonlinelibrary.com](http://wileyonlinelibrary.com).]

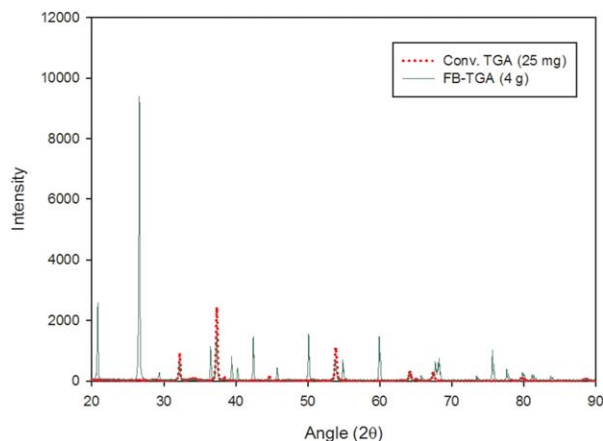


**Figure 10. XRD results of the treated samples from Conv. TGA and FB-TGA.**

[Color figure can be viewed in the online issue, which is available at [wileyonlinelibrary.com](http://wileyonlinelibrary.com).]

Conversely, the results obtained from 4 g of  $\text{Ca}(\text{OH})_2$  in the fluidized bed TGA are in agreement with those obtained from 25 mg of  $\text{Ca}(\text{OH})_2$  in the conventional TGA but only during the first zone. In fact, only one stage for the thermal decomposition of  $\text{Ca}(\text{OH})_2$  in the FB-TGA can be considered (360–540°C).

These results suggest that, in the case of FB-TGA, it is quite likely that the thickness of  $\text{CaO}(\text{s})$  shell layer would be less than that in the case of fixed, conventional bed TGA due to spalling of the  $\text{CaO}(\text{s})$  shell layer in the FB-TGA. This affects both the heat and species mass transfer resistances. Also, the effect of turbulence in the FB-TGA would be to decrease the effective thickness of the gas film (or, concentration boundary layer) around the particle. Its effect on the intraparticle diffusion mass-transfer coefficient would be negligibly small, if any. One way to minimize or eliminate the effect of intraparticle diffusion mass transfer of a species, such as water vapor, is to decrease the solid  $\text{Ca}(\text{OH})_2$  particle size so that the concentration of water vapor as a function of the radial distance in the particle pores is almost flat.

In addition, the obtained samples were analyzed by x-ray diffraction (XRD). The results are demonstrated in Figure 10. The scores for  $\text{Ca}(\text{OH})_2$  are 26 for the sample treated in the conventional TGA (25 mg) and three for the one treated in FB-TGA. These results confirm that (1) the effective thickness of the gas film around the particle was greatly decreased, and (2) the intraparticle diffusion of  $\text{H}_2\text{O}$  throughout the formed layer of  $\text{CaO}$  was relatively suppressed in the case of the FB-TGA. Consequently, the heat and water vapor mass transfer were significantly enhanced using the FB-TGA.

Furthermore, the overall decomposition of  $\text{Ca}(\text{OH})_2$  in the FB-TGA was 75.4%. This experimental value, obtained from the FB-TGA, is in perfect agreement with the calculated value (75.6%) from the decomposition reaction of dry  $\text{Ca}(\text{OH})_2$ , which confirms the reliability and the repeatability of the newly developed FB-TGA.

## Conclusion

To provide accurate and more comprehensive kinetic models for gas-solid reactions, the FB-TGA was developed. The standard equipment was validated and applied to calcium

oxide decomposition. The experiments demonstrated that FB-TGA provided good and more reliable results for the thermal decomposition of  $\text{Ca}(\text{OH})_2$  than the conventional TGA. Bulk and interparticle diffusion were perfectly suppressed by the application of FB-TGA. The treated samples were analyzed by XRD and the results confirmed that, by applying the FB-TGA, both heat and species mass transfer limitations were almost eliminated.

Studying kinetics and the mechanism of catalytic pyrolysis, combustion and gasification of coal, biomass, and waste solid in the newly developed FB-TGA are in progress, and the results will be published in the near future.

## Notation

- $U_g$  = superficial Gas velocity, m/s
- $U_{mf}$  = minimum fluidization velocity, m/s
- $m_{\text{sand}}$  = mass of sand, kg
- $m_{\text{bed}}$  = mass of bed, kg
- $\Delta P_{\text{dist.}}$  = pressure drop across the distributor, Pa
- $\Delta P_{\text{bed}}$  = pressure drop across the bed, Pa
- $\Delta P_{\text{filter}}$  = pressure drop across the filter, Pa
- $\Delta P_{mf}$  = pressure drop across the bed at minimum fluidization, Pa
- $S$  = transversal area of the reactor,  $\text{m}^2$
- $U_{g0}$  = gas velocity at the inlet of the distributor, m/s
- $U_{g1}$  = gas velocity at the outlet of the distributor, m/s
- $U_{g2}$  = gas velocity at the inlet of the filter, m/s
- $U_{g3}$  = gas velocity at the outlet of the filter, m/s
- $g$  = gravity acceleration,  $\text{m}^2/\text{s}$
- $\Delta m_p$  = pseudo variation of the weight of the reactor, kg
- $\alpha_p$  = pressure drop to weight conversion factor,  $\text{kg}/\text{Pa}$

## Literature Cited

- Yu J, Yue J, Liu Z, Dong L, Xu G, Zhu J, Duan Z, Sun L. Kinetics and Mechanism of Solid Reactions in a Micro Fluidized Bed Reactor. *AIChE J.* 2010;56(11):2905–2912.
- Pantoya M, Granier JJ, Rai A, Park K, Zachariah M. The effect of heating rate on the reaction kinetics of nanoscale aluminothermic reaction. *AIChE Annual Meeting and Fall Showcase, Conference Proceedings.* 2005:3237.
- Despina V, Evaggelia K, Stelios S, Piero S. Gasification of waste biomass chars by carbon dioxide via thermogravimetry-effect of catalysts. *Combust Sci Technol.* 2012;184:64–77.
- Katarzyna S, Pietro B, Francesco F. Thermogravimetric analysis and kinetic study of poplar wood pyrolysis. *Appl Energy.* 2012;97:491–497.
- Sanders JP, Gallagher PK. Kinetics of the oxidation of magnetite using simultaneous TG/DSC. *J Therm Anal Calorim.* 2003;72(3):777–789.
- Sivakumar P, Sivakumar P, Anbarasu K, Mathiarasi R, Renganathan S. An eco-friendly catalyst derived from waste shell of scylla tranquebarica for biodiesel production. *Int J Green Energy.* 2014;11(8):886–897.
- Yılgin M, Duranay ND, Pehlivan D. Co-pyrolysis of lignite and sugar beet pulp. *Energy Conversion Manage.* 2010;51:1060–1064.
- Wang F, Zeng X, Han J-Z, Zhang J-W, Liu Y-Y, Wang Y, Li A-M, Yu J, Xu G-W. Comparison of char gasification kinetics studied by micro fluidized bed and by thermogravimetric analyzer. *J Fuel Chem Technol.* 2013;41(4):407–413.
- Radmanesh R, Courbariaux Y, Chaouki J, Guy C. A unified lumped approach in kinetic modeling of biomass pyrolysis. *Fuel.* 2006;85(9):1211–1220.
- Yu J, Yao C, Zeng X, Geng S, Dong L, Wang Y, Gao S, Xu G. Biomass pyrolysis in a micro-fluidized bed reactor: characterization and kinetics. *Chem Eng J.* 2011;168(2):839–847.
- Yu J, Zeng X, Zhang J, Zhong M, Zhang G, Wang Y, Xu G. Isothermal differential characteristics of gas-solid reaction in micro-fluidized bed reactor. 2013;103:29–36.
- Lin Y-h, Guo Z-c, Tang H-g, Ren S, Li J-w. Kinetics of reduction reaction in micro-fluidized bed. *J Iron Steel Res Int.* 2012;19(6):6–8.
- Ebrahimpour O, Chaouki J, Dubois C. Diffusional effects for the oxidation of SiC powders in thermogravimetric analysis experiments. *J Mater Sci.* 2013;48(12):4396–4407.

Manuscript received Feb. 25, 2014, and revision received Aug. 25, 2014.